tvst

Retina

Computational Fluid Dynamics Modeling of Intravitreal Ranibizumab Bolus Versus Subretinal ABBV-RGX-314 Transgene Product in Human Eyes

Jenny Park[1], Mohammad Kazemi[2], Mitalee Tamhane[1], and Jie Shen[1]

[1] AbbVie, Clinical Pharmacology, Irvine, California, USA
[2] Independent Consultant, San Jose, California, USA

Correspondence: Jie Shen, AbbVie, Clinical Pharmacology, 2525 Dupont Drive, Irvine, CA 92612, USA. e-mail: shenj@abbvie.com

Received: January 29, 2025
Accepted: August 2, 2025
Published: October 3, 2025

Keywords: nAMD; gene therapy; pharmacokinetic; modeling

Citation: Park J, Kazemi M, Tamhane M, Shen J. Computational fluid dynamics modeling of intravitreal ranibizumab bolus versus subretinal ABBV-RGX-314 transgene product in human eyes. Transl Vis Sci Technol. 2025;14(10):6, https://doi.org/10.1167/tvst.14.10.6

Purpose: ABBV-RGX-314 is being developed for neovascular age-related macular degeneration (nAMD). Computational fluid dynamics (CFDs) modeling in the eye enables simulation of drug distribution incorporating geometry and substructures of the eye across species. Given the similarity between ranibizumab and ABBV-RGX-314 transgene product (TP), ranibizumab intraocular pharmacokinetic (PK) data from literature were used to simulate intraocular drug distribution of ABBV-RGX-314 TP. This investigation aims to use CFD modeling to estimate retinal TP level based on aqueous humor (AH) TP level following subretinal (SR) injection of ABBV-RGX-314 in patients with nAMD.

Methods: Ocular distribution of ranibizumab following a single intravitreal (IVT) injection was modeled in both monkey and human eyes independently. Following model validation, ABBV-RGX-314 TP distribution in human eyes was simulated following retinal transduction of ABBV-RGX-314.

Results: Iterative simulations were performed to achieve similar AH ABBV-RGX-314 TP levels in patients with nAMD from phase I/IIa Study RGX-314-001. The CFD simulation estimated corresponding retinal TP concentrations of 1.86 to 5.50 µg/g at steady-state, which was assumed to be reached by 28 days and falls within the range of the estimated retinal ranibizumab trough retinal ranibizumab concentration (C_{trough}; 0.718–5.37 µg/g) following monthly and every other month (EOM) dosing of 0.5 mg ranibizumab in patients with nAMD.

Conclusions: The current study results predict that the 2 pivotal trial ABBV-RGX-314 doses (6.4E10 and 1.3E11 genome copies/eye) are expected to achieve and maintain sufficient retinal ABBV-RGX-314 TP levels for the treatment of nAMD.

Translational Relevance: CFD modeling effectively bridges limited human ocular PK data with rich preclinical data, supporting model-informed drug development (MIDD) for clinical dose selection.

Introduction

Neovascular age-related macular degeneration (nAMD) accounts for approximately 10% to 15% of all AMD cases and is one of the leading causes of severe vision loss in the elderly population.[1] Although the cause of the disease is multifactorial, it is primarily characterized by an overproduction of vascular endothelial growth factor (VEGF) leading to pathological choroidal neovascularization.[2,3] This abnormal development of immature blood vessels results in accumulation of blood and fluid underneath the central region of the retina known as the macula, causing inflammation, obscuring central vision, and ultimately leading to severe loss of vision if left untreated. Given the central role of VEGF in the pathogenesis of nAMD, anti-VEGF agents have become the mainstay treatment for nAMD.[4] However, one major drawback associated with the approved anti-VEGF therapies is the frequent intravitreal (IVT) injections necessary to maintain clinical benefit, which

pose a significant treatment burden to the patients, caregivers, and the health care system. Although more recently approved anti-VEGF therapies, such as VABYSMO (Genentech) and Eylea HD (Regeneron), have extended the dosing intervals to as long as 16 weeks, a one-time administration gene therapy that could potentially eliminate or reduce the IVT injection burden by providing longer lasting efficacy continues to hold great appeal.

ABBV-RGX-314 is an investigational AAV8 vector-based gene therapy product that contains a transgene encoding a soluble monoclonal anti-VEGF antibody fragment (Fab), similar in structure, molecular weight, and biological activity to ranibizumab (Lucentis; Genentech).[1] One of the ways this is being developed is for the treatment of nAMD with subretinal (SR) route of administration. This investigational gene therapy utilizes a biofactory approach by harnessing the eye's own cells to produce a sustained supply of therapeutic protein and offers an alternative approach to treating retinal diseases. In contrast to IVT, which is the route of administration for several other gene therapy drug candidates to treat retinal diseases, an SR injection delivers the gene therapy product directly to the target cells, such as retinal pigment epithelium and photoreceptors, for effective transduction and transgene expression leading to localized biological activity of the transgene product (TP).

Characterizing drug exposure in the ocular tissues, particularly the retina, is critical to understanding the exposure-response relationship in patients with nAMD and to optimizing dose in clinical trial designs. For drugs treating retinal diseases, the intra-ocular pharmacokinetic (PK) profile can be assessed via sampling of aqueous humor (AH) in the anterior segment of the eye.[1,5–8] Although AH is a good surrogate matrix to confirm successful transduction of a gene therapy product delivered in the SR space, drug levels sampled from this compartment may not directly reflect drug levels in the retina given the anatomic and hydrodynamic barriers for drug distribution from the retina to the anterior segment and back. Therefore, there is a need for a sophisticated translational model built using rich nonclinical ocular PK data collected from extensive sampling across various ocular tissues and translate to humans. Computational fluid dynamics (CFDs) modeling in the eye allows simulation of drug distribution based on known drug physicochemical properties and permeability across tissue layers, whereas incorporating geometry and substructures of the eye across species. This modeling approach has been applied to gain insights into drug exposure in tissues of the human eye that are not readily available for assessment, such as the retina.[9]

In this investigation, literature reported ocular ranibizumab PK data in humans and monkeys following IVT administration were leveraged to calibrate and validate the ocular CFD model. Given the similarity in amino acid sequences between the soluble anti-VEGF Fab (ABBV-RGX-314 TP) produced as a result of retinal transduction of ABBV-RGX-314 and ranibizumab, parameters used to build and calibrate the ocular CFD model for IVT ranibizumab were utilized to simulate the distribution of ABBV-RGX-314 TP across various ocular compartments following SR injection of ABBV-RGX-314. The primary objective of this investigation was to leverage the AH ABBV-RGX-314 TP data from the phase I/IIa dose escalation study (RGX-314-001) to derive the corresponding retinal ABBV-RGX-314 TP concentration through CFD modeling to assess sufficiency of the retinal drug exposure in patients with nAMD.

Methods

A summary of the published PK data utilized in the calibration and validation of the ocular CFD model is presented in Table 1.

CFD Simulations

Three-dimensional (3D), transient simulations were conducted for both monkey and human[10] eyes using ANSYS FLUENT software (2024-R1 release). The model for each species included half of the eye (Fig. 1) as symmetry-plane boundary condition (BC) was applied on the half-plane boundary. Each eye model included AH, vitreous humor (VH), retina, choroid, sclera, cornea, lens, iris, ciliary body (CB), and trabecular meshwork (TM) regions. Schlemm's canal, tear, lids, and glands were disregarded in the eye model. However, the clearance of drug that was removed through the Schlemm's canal and tear was modeled by applying a BC of zero drug concentration on the outlet boundary of TM and the top surface boundary of the cornea. In addition, eyeball motion was not considered in the present simulation work. For simplification, the lens and iris were assumed to behave as solid domains, where AH fluid does not permeate through them. The AH flow was produced by the CB and permeates the anterior chamber. The AH, VH, retina, choroid, sclera, and cornea regions were treated as porous fluid domains where AH fluid permeates through them. The viscous resistance values for these regions are listed in Table 2.[9] CFD simulations were first conducted to determine the velocity of

Table 1. Summary of Study Design Parameters From Publications Used in the CFD Modeling

	Gaudreault et al.[12]	Krohne et al.[5]	Campochiaro et al.[1]
N	Cynomolgus monkeys	Humans	Humans
Sample size	6	18	42
Drug	Ranibizumab	Ranibizumab	ABBV-RGX-314
Analyte	Ranibizumab	Ranibizumab	ABBV-RGX-314 TP
Dose	0.5 mg	0.5 mg	Cohort 3: 6.0×10^{10} GC/eye Cohort 4: 1.6×10^{11} GC/eye
Administration route	IVT	IVT	SR
Injection volume	50 µL	50 µL	250 µL
Sampled matrices	Vitreous humor Aqueous humor Retina	Aqueous humor	Aqueous humor

GC, genome copies; IVT, intravitreal; SR, subretinal; TP, transgene product.

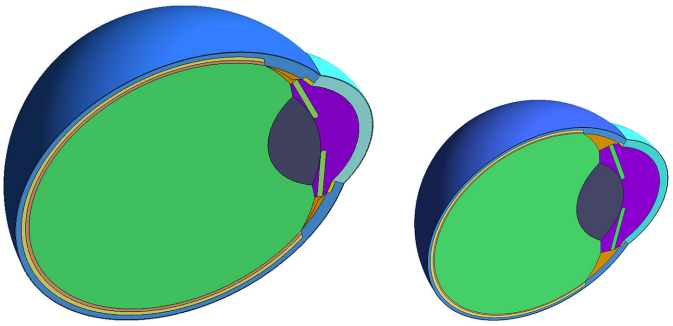

Figure 1. Illustration of the geometry for the human eye (*left*) and the monkey eye (*right*) shown to scale.

Table 2. Viscous Resistance Values for Various Regions in Human and Monkey Eyes

	Viscous Resistance [1/m^2]	
Region	Human Eye	Monkey Eye
Aqueous humor	0	0
Vitreous humor	1.19E+13	1.19E+13
Cornea and sclera	6.67E+17	6.67E+17
Retina and choroid	6.67E+17	6.67E+17
Trabecular meshwork	6.33E+15	6.46E+15

The viscous resistance values for all regions, except for TM region, were adopted from Missel et al.[9]

AH fluid across different regions that originated from CB and drained out to TM. The resulting pressure of AH fluid was also determined across various regions.

The AH flow rate was set to 2.4 µL/min for a human eye and 2.0 µL/min for a monkey eye.[11] These AH flow rates were applied as BCs at the CB. The relative pressure on the outer surfaces of the cornea and sclera were set to 0 millimeters of mercury (mm Hg) and 10 mm Hg, respectively, for both human and monkey eyes.[9] Assuming normotension, the intraocular pressure (IOP) was set to 15 mm Hg for both human and monkey eyes. Darcy's law was used to model the AH flow in the porous regions. It should be noted that the viscous resistance values for all regions except for TM were taken from a previous literature report.[9] The viscous resistance for TM was determined iteratively, via simulations, by targeting an IOP value of 15 mm Hg for both human and monkey eyes.[9] The density and viscosity of AH fluid was set to 1000 kg/m^3 and 0.001 kg/m.sec, respectively, representing water properties at 37°C.

Computational Simulations of Ranibizumab Movement

Upon completion of CFD simulations, ranibizumab movement simulations were conducted, allowing the drug to be transported via a combination of advection and diffusion mechanisms. The flow diagram summarizing the CFD modeling approach is shown in Figure 2.

First, simulations of ranibizumab intraocular distribution were conducted with a single bolus IVT injection of 0.5 mg ranibizumab in both human and monkey eyes. At time 0, the 0.5 mg IVT bolus was assumed to be of a spherical shape (radius = 2.285 mm) at a volume of 50 µL, resulting in the initial ranibizumab vitreous concentration (C_0) of 10,000 µg/mL within the bolus sphere and 0 µg/mL elsewhere (Fig. 3A). Over time, ranibizumab moves to adjacent regions via diffusion and advection mechanisms. Figure 3B illustrates the ranibizumab concentration in human and monkey eyes at day 30 post-dose. The results of the simulations were compared against the published experimental data in

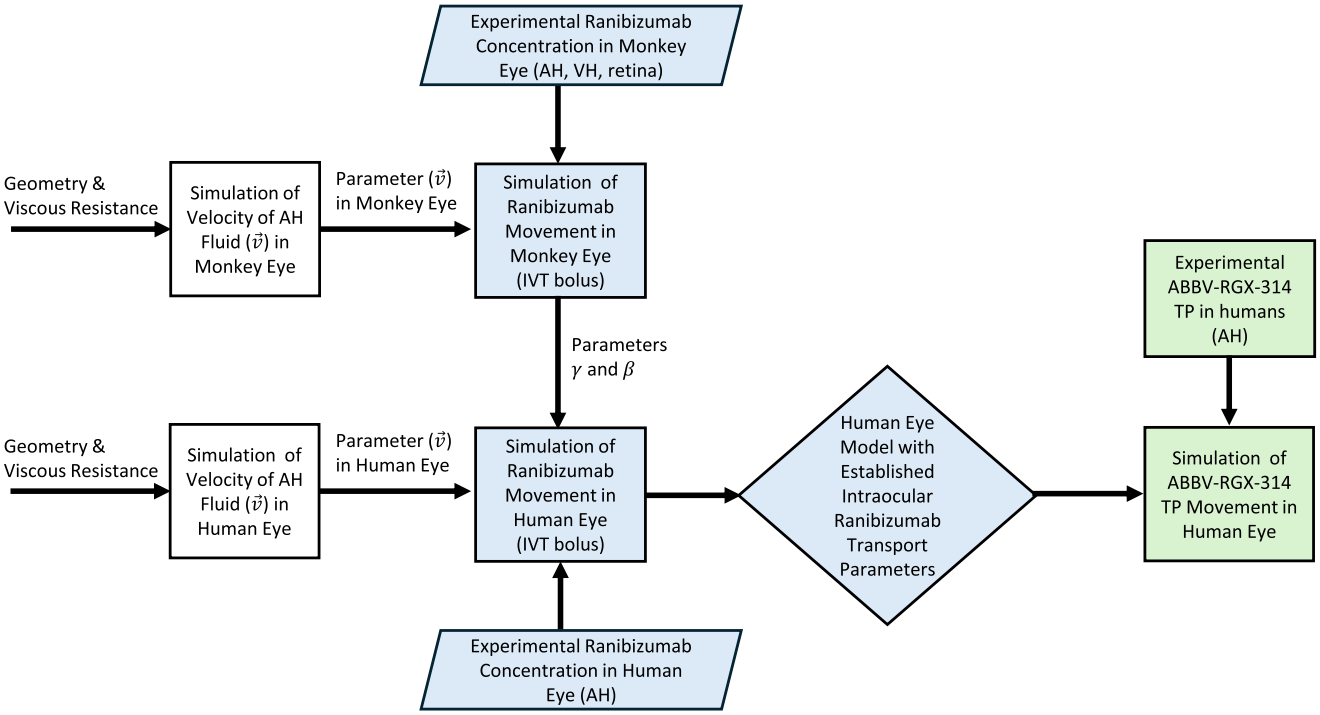

Figure 2. A flow diagram of computational fluid dynamics (CFD) modeling approach. AH, aqueous humor; β, coefficient for diffusion coefficient; γ, coefficient for sink term; IVT, intravitreal; SR, subretinal; TP, transgene product; VH, vitreous humor.

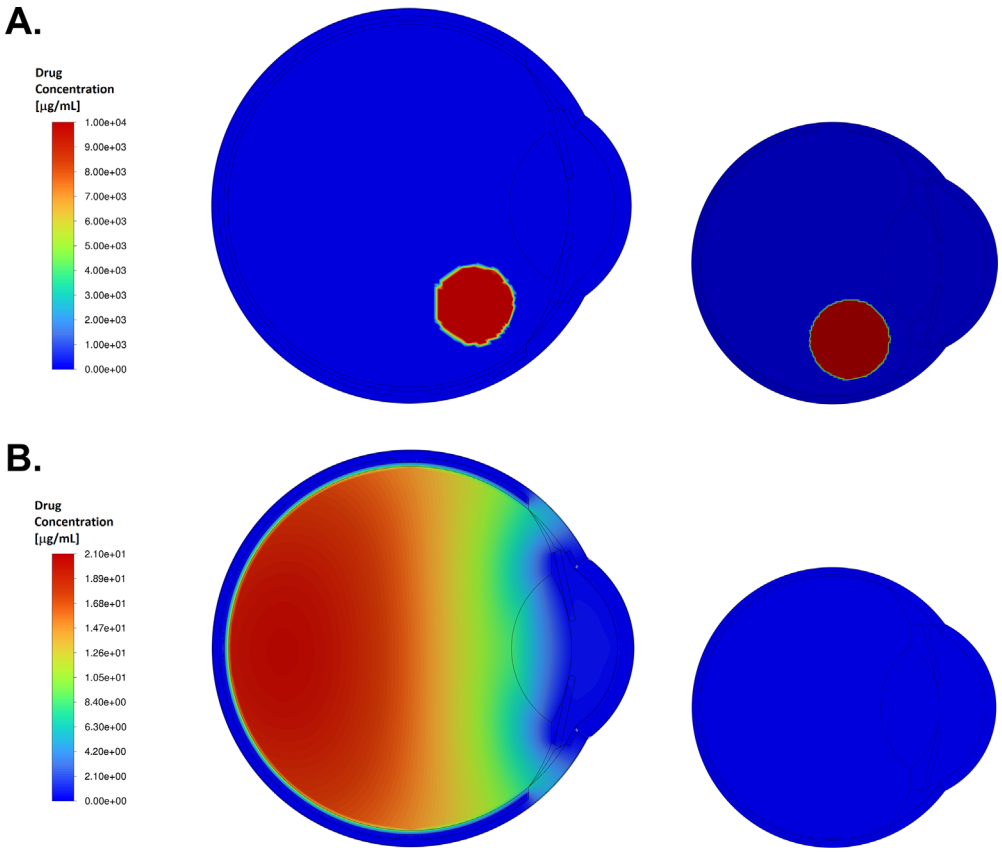

Figure 3. Contour plot of (**A**) initial ranibizumab concentration (t = 0 seconds) following a 0.5 mg IVT bolus injection of ranibizumab and (**B**) ranibizumab concentration 30 days post-dose on the symmetry plane of the human eye (*left*) and the monkey eye (*right*).

human and monkey eyes and the inputs were adjusted to calibrate the model.[5,12]

After calibration, simulations of ABBV-RGX-314 TP following retinal transduction were conducted in human eyes, assuming homogeneous transduction of ABBV-RGX-314 in the entire retina resulting in continuous ABBV-RGX-314 TP expression. Key parameters (diffusion coefficients and sink term) derived based on the calibrated human CFD model with ranibizumab bolus IVT dosing were applied to simulate the ABBV-RGX-314 TP distribution due to similarities in the amino acid sequence and thereby molecular weights between the 2 drugs. It was assumed that, upon SR injection of ABBV-RGX-314, the steady-state level of ABBV-RGX-314 TP expression in the retina is achieved by 28 days post administration, which is a typical time to reach steady-state transgene expression for AAV-based gene therapies, and remains constant thereafter to account for time to reach steady-state.[13,14] The lack of significant difference in AH ABBV-RGX-314 TP levels observed at 1 and 6 months in cohort 3 of the phase I/IIa study (RGX-314-001) supports this assumption.[1] Furthermore, for simplification, the model did not account for any prior or supplemental ranibizumab injection.

The movement of drug in the eye was assumed to be governed by advection and diffusion mechanisms, as described by the transportation Equation 1:

$$\frac{\partial \emptyset}{\partial t} + \vec{\mathbf{v}} \cdot \nabla \emptyset = D\nabla^2 \emptyset + S \quad (1)$$

In this equation, $\emptyset$ is the drug concentration, $\frac{\partial \emptyset}{\partial t}$ represents the temporal term, $\vec{\mathbf{v}} \cdot \nabla \emptyset$ is the advection term, $D\nabla^2 \emptyset$ represents the diffusion term, and S represents the sink term. The sink term modeled the drug uptake by the choroid and was set to be zero elsewhere. The drug concentration ($\emptyset$) at any location in the eye and at any given time can be estimated by solving the transportation equation if velocity of AH fluid ($\vec{\mathbf{v}}$) and the diffusion coefficient of the formulation (D) are numerically defined. The diffusion coefficients in each compartment were assumed to be homogenous within that ocular compartment. It should be noted that velocity of AH fluid ($\vec{\mathbf{v}}$) was determined via CFD simulations, whereas the diffusion coefficients of ranibizumab (D) in various regions of the eye were specified as an input for the simulations. The diffusion coefficient of ranibizumab in AH was calculated using the Equation 2 suggested by Torres et al.[15]:

$$D = \beta M^{-1/3} \quad (2)$$

Where, in this equation, D is the diffusion coefficient in the m^2/sec unit, M is the molecular mass in the Da unit, and β is the coefficient for diffusion coefficient.[15] The coefficient β ($\beta = 8.0E{-}09$) was derived by calibrating the bolus IVT ranibizumab simulation results with published monkey and human ocular PK data.[5,12] Based on the molecular weight of ranibizumab (48.35 kilodalton [kDa]), the diffusion coefficient in AH was calculated to be 1.37×10^{-10} m^2/sec.[16] This value is comparable to Hutton-Smith et al.'s calculation of the diffusion coefficient of ranibizumab in physiological saline (1.34×10^{-10} m^2/sec).[17] Table 3 lists the diffusion coefficients of ranibizumab estimated in various regions using the methodology proposed by Missel.[9]

Table 3. Diffusion Coefficients of Ranibizumab in Various Regions of Human and Monkey Eyes Estimated Using the Methodology Proposed by Missel[9]

Region	Diffusion Coefficient [m^2/s]
Aqueous humor	1.37E-10
Vitreous humor	4.57E-11
Cornea and sclera	1.03E-11
Retina and choroid	1.03E-12
Iris and ciliary body	4.57E-11
Lens	2.29E-11
Trabecular meshwork	1.03E-11

As Schlemm's canal was absent in the model, the drug drained from the Schlemm's canal was modeled by setting the drug concentration to zero at the outlet boundary of TM. Similarly, the clearance of the drug by the tear on cornea surface boundary was modeled by setting the drug concentration to zero on the top surface of cornea. Uptake of the drug by the choroidal vasculature was modeled using a sink term (term S in Equation 1) and was expressed as follows in Equation 3[18]:

$$S = -\gamma \times \emptyset \quad (3)$$

In this equation, γ ($\gamma = 0.2$) is the coefficient for the sink term and was determined by calibrating the simulated bolus IVT ranibizumab concentration result against published monkey and human ocular PK data.[5,12]

Following the approach described by Tojo and Isowaki, a partition coefficient was applied at the interface between tissues to model drug distribution and binding across different tissue regions.[19] The partition coefficient of 0.5 for ranibizumab was defined at the interfaces of vitreous to retina, retina to choroid, and choroid to sclera which was determined to ensure good agreement between simulation results and published monkey and human ocular PK data.[5,12] The partition

coefficients derived from available experimental data in monkey eyes were assumed to hold constant in human eyes.

Simulation of ABBV-RGX-314 TP (anti-VEGF Fab) in Human Eye Utilizing Ranibizumab CFD Model

A phase I/IIa dose-escalation study of ABBV-RGX-314 by SR route of administration was conducted in patients with nAMD (RGX-314-001; NCT03066258) and the key study design features and findings have been published by Campochiaro et al.[1] Briefly, this study evaluated the efficacy, safety, pharmacodynamics (ABBV-RGX-314 TP), and vector shedding of a single SR dose of ABBV-RGX-314 gene therapy in patients with nAMD up to 2 years. A total of 42 patients received 1 of 5 escalating doses ranging from 3.0×10^9 genome copies per eye (GC/eye) to 2.5×10^{11} GC/eye, with each cohort consisting of 6 to 12 patients. During the active run-in, patients received an IVT ranibizumab (0.5 mg) injection 2 weeks prior to the ABBV-RGX-314 treatment. Thereafter, PRN ranibizumab was permitted beginning 4 weeks post ABBV-RGX-314 administration if prespecified supplemental anti-VEGF injection criteria were met. To assess ABBV-RGX-314 biological activity in the eye, ABBV-RGX-314 TP (anti-VEGF Fab) levels were measured in AH samples throughout the study, including at 1 month, 6 months, 1 year, and 2 years, and quantified using a qualified bioanalytical method. In this study, ABBV-RGX-314 TP concentrations in AH increased in a dose-dependent manner, with maximum TP expression occurring approximately 6 months post-dose. At 6 months and 2 years, the mean AH ABBV-RGX-314 TP concentrations in cohort 3 (6.0×10^{10} GC/eye) were 217.8 ng/mL ($n = 6$) and 227.2 ng/mL ($n = 6$), respectively, and in cohort 4 (1.6×10^{11} GC/eye) were 643.8 ng/mL ($n = 10$) and 272.8 ng/mL ($n = 11$), respectively. These two doses bracket the doses being tested in two ongoing pivotal trials for ABBV-RGX-314 in nAMD (6.4×10^{10} GC/eye and 1.3×10^{11} GC/eye; ATMOSPHERE [NCT04704921] and ASCENT [NCT05407636]).

Given the similarity in amino acid sequences and thereby molecular weights between ABBV-RGX-314 TP and ranibizumab, clinical ABBV-RGX-314 TP AH concentration data from the phase I/IIa study was leveraged to simulate ABBV-RGX-314 TP ocular distribution profile following retinal transduction in human eyes using the CFD model developed for ranibizumab.

To evaluate whether sufficient retinal exposure of ABBV-RGX-314 TP was achieved in human eyes, the peak AH ABBV-RGX-314 TP concentration of 643.8 ng/mL observed in cohort 4 at 6 months (rounded up to the nearest hundreds, 700 ng/mL) in study RGX-314-001, it was chosen as the steady-state AH drug concentration.[1] Iterative simulations of ABBV-RGX-314 TP concentration-time profiles in AH, VH, and retina were then performed for 180 days post-dose administration.

Results

CFD Simulation

Figure 4 illustrates the contour plots of pressure (see Fig. 4A) and velocity of AH fluid (see Fig. 4B) on the symmetry-plane of human and monkey eyes, respectively, based on CFD simulation results. The velocity of AH fluid in the front of the eye was much greater than that in the back of the eye in both species. This finding suggests that the advection mechanism of drug movement in the anterior segment of the eye is relatively stronger than that in the posterior segment of the eye. It was found that the pressure in most regions of the eye was between 10 mm Hg and 15 mm Hg, and a sharp decline of pressure was observed across the cornea.

Simulations of IVT Bolus Ranibizumab

The intraocular distribution of ranibizumab following a single IVT bolus injection was simulated in both human and monkey eyes using the CFD model.

Figure 5 compares the simulated concentration-time profiles of ranibizumab in the AH (see Fig. 5A), the VH (see Fig. 5B), and the retina (Fig. 5C), and experimental data in the monkey eye, showing good agreement between the two datasets in all three matrices (AH: $R^2 = 0.707$, VH: $R^2 = 0.970$, and retina: $R^2 = 0.944$).[12]

The parameters (γ and β), which represent coefficients of drug uptake by the choroid and the calibration coefficient for the diffusion coefficient, respectively, derived from the calibrated CFD model for monkey eyes were assumed to hold constant across species and applied to build the human ocular CFD model for IVT ranibizumab. Overall, the simulated AH PK profile is in general agreement with the published AH data in humans following a single dose IVT administration of 0.5 mg ranibizumab ($R^2 = 0.505$; Fig. 6A).[5] Limited observed human ocular PK data, particularly at early timepoints where concentrations are antici-

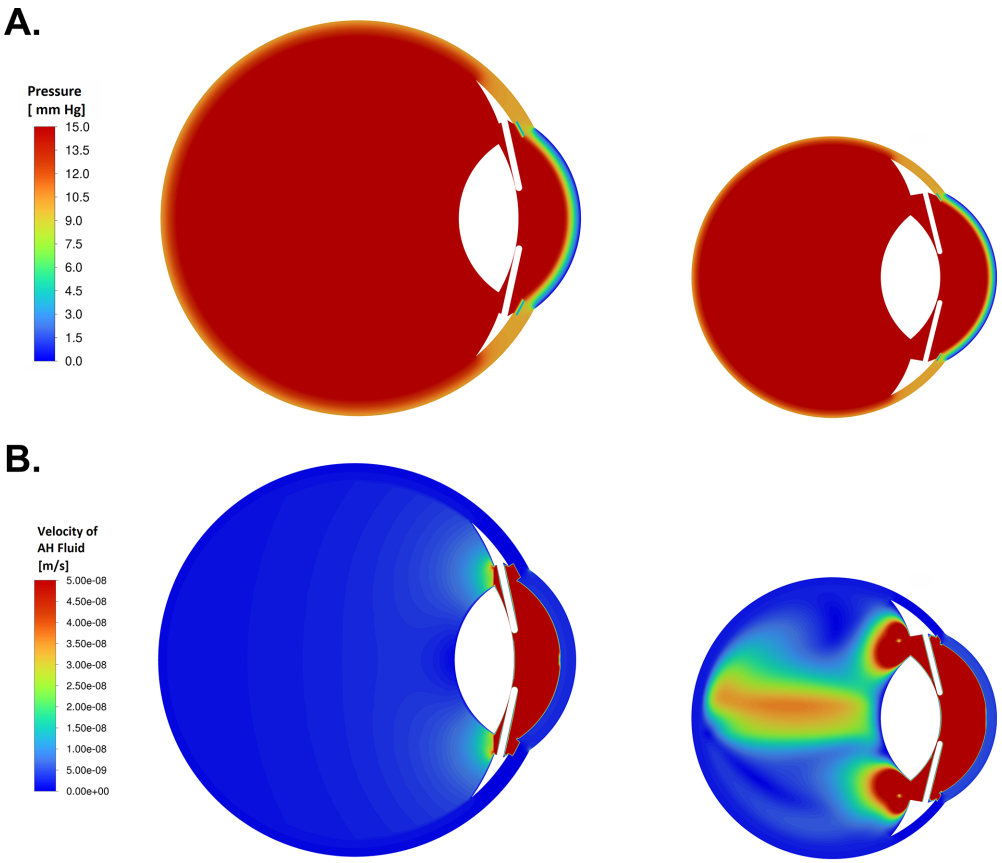

Figure 4. Contour plots of pressure (mm Hg) (**A**) and velocity of AH fluid (m/s) (**B**) on the symmetrical plane of the human eye (*left*) and the monkey eye (*right*) based on CFD simulations.

pated to be high, and high variability in the observed ocular PK data likely explain the poor model fit to the reported ocular PK data. Figure 6B illustrates the CFD model simulated ranibizumab concentration-time profiles in the VH, AH, and retina of a human eye. Given the IVT route of administration, ranibizumab concentration was the highest in the VH, followed by the retina and AH. The simulated AH ranibizumab concentration rapidly reached its peak concentration of 121 µg/mL at approximately the 17th hour post-dose and declined monoexponentially to 2.74 µg/mL by day 30. The retina to VH concentration ratio reached an asymptotic level of 0.36 in approximately 10 days, which is similar to the ratio of 0.32 based on the area under the curve from 0 to infinity ($AUC_{0\text{-}\infty}$) between the retina and VH determined in nonhuman primates (NHPs).[12] Based on this simulation, the trough retinal ranibizumab concentration (C_{trough}) at day 30 post-dose (following monthly bolus IVT administration of 0.5 mg ranibizumab per Lucentis product label) is 5.37 µg/g and 0.718 µg/g at day 56 post-dose (assuming once every 8 weeks [Q8W] dosing).

Simulations of ABBV-RGX-314 TP Following Retinal Transduction

Given the agreement between the experimental and simulated ranibizumab ocular PK data following bolus IVT administration in both species, the CFD model was then adopted for SR administration of ABBV-RGX-314 in the human eye. The contour plot in Figure 7 illustrates the steady-state concentration of ABBV-RGX-314 TP in the human eye at the end of 180-day simulation. ABBV-RGX-314 TP was assumed to be expressed throughout the entire retinal region and spread throughout the eye at steady-state. Figure 8 depicts the simulated ABBV-RGX-314 TP concentration-time profiles in the VH, AH, and retina in humans. This simulation estimated retinal ABBV-RGX-314 TP concentration of 5.98 µg/g to achieve AH TP concentration of 700 ng/mL. Using this model, the simulated retinal ABBV-RGX-314 TP concentrations based on the observed AH ABBV-RGX-314 TP concentrations in patients with nAMD receiving 6.0×10^{10} GC/eye (cohort 3) and 1.6×10^{11} GC/eye (cohort 4) in Study RGX-314-001 were

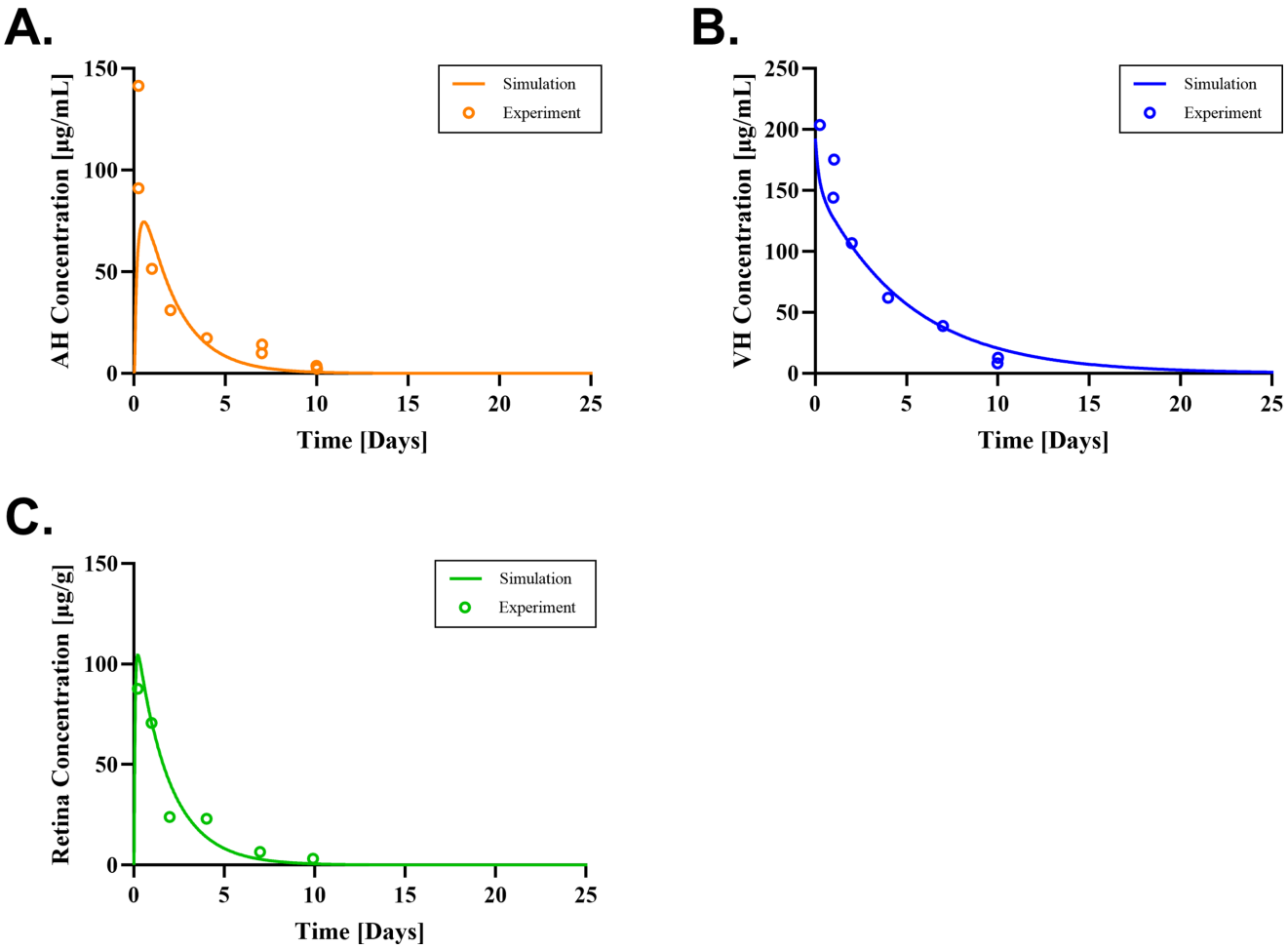

Figure 5. Simulated versus experimental[12] ranibizumab concentration-time profiles in (**A**) the AH ($R^2 = 0.707$), (**B**) the VH ($R^2 = 0.970$), and (**C**) the retina ($R^2 = 0.944$) of the monkey eye following a single IVT bolus injection of 0.5 mg ranibizumab.[12] AH, aqueous humor; IVT, intravitreal; VH, vitreous humor.

1.86 µg/g and 5.50 µg/g, respectively, at 6 months post-dose.

Discussion

The model-informed drug development (MIDD) approach has been described as a powerful quantitative tool particularly in the development of ocular gene therapy. It has the potential to inform dose selection and trial design optimization and to support the evaluation of safety and efficacy profiles.[20] There is a growing interest from various regulatory agencies, including the United States Food and Drug Administration (FDA), to develop frameworks focused on advancing MIDD in hopes of facilitating the drug development process and regulatory reviews, while substantially saving time and costs.[21,22] The CFD model described in this investigation integrated the complexity of different ocular compartments with the molecular properties of ranibizumab to simulate the intraocular distribution of ranibizumab following a single IVT bolus dose of ranibizumab and ABBV-RGX-314 TP following SR administration of ABBV-RGX-314. Overall, the model simulation showed a reasonably good fit to the published experimental IVT ranibizumab ocular PK data in both monkey and human eyes. Based on this agreement, the model was adopted to simulate TP distribution following treatment with the gene therapy product.

As expected, simulations of a single IVT administration of ranibizumab resulted in an initial high peak concentration followed by a rapid decline in human retina. Monthly dosing with IVT ranibizumab is likely needed due to this rapid decline in ranibizumab concentrations in the target ocular compartment and may explain fluctuations in best-corrected visual acuity

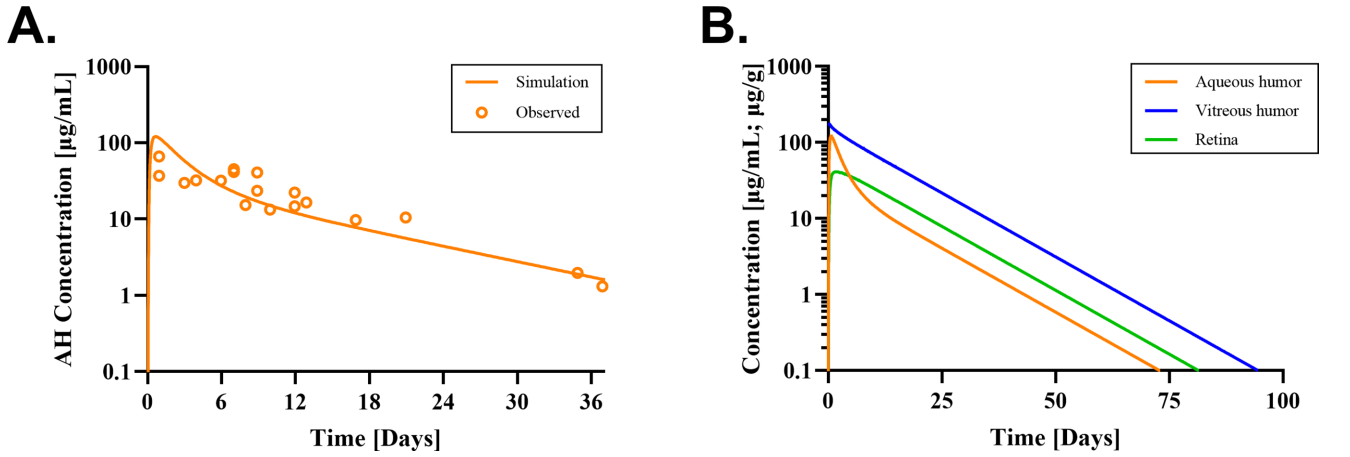

Figure 6. Simulated ranibizumab concentration-time profiles (**A**) overlaid with experimental AH ranibizumab data[5] ($R^2 = 0.505$) and (**B**) in the AH, VH, and retina in the human eye following a single IVT bolus injection of 0.5 mg ranibizumab.[5] AH, aqueous humor; IVT, intravitreal; VH, vitreous humor.

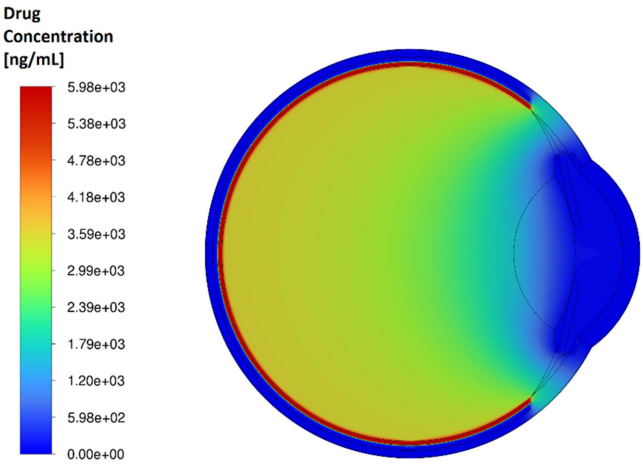

Figure 7. Contour plot of ABBV-RGX-314 TP concentrations at steady-state (t = 180 days) on the symmetry plane of the human eye.

(BCVA) reported in the literature with off label treatment regimens, such as treat-and-extend (T&E) or pro re nata (PRN).[23,24] This well-documented fluctuating patterns of BCVA in response to repeat IVT anti-VEGF treatment suggest that the C_{trough} of anti-VEGF therapies (ranibizumab) is likely important for optimal efficacy. Comparatively, gene therapy products with a biofactory approach, such as ABBV-RGX-314, are designed to achieve prolonged and steady exposure of the therapeutic protein in the target tissues without the need for frequent IVT injections. This is evidenced by the recent publication of the 2-year results of the phase I/IIa dose escalating study of ABBV-RGX-314 in patients with nAMD (RGX-314-001), which demonstrated the expression of ABBV-RGX-314 TP up to 2 years after SR injection in all dose cohorts.[1] The sustained AH ABBV-RGX-314 TP expression was accompanied by maintenance or improved (gain >5 Early Treatment Diabetic Retinopathy Study [ETDRS] letters) mean BCVA and mean central retinal thickness (CRT) over 2 years with reduced annualized supplemental anti-VEGF injection rates at doses of 6×10^{10} GC/eye and higher (mean 1-year annualized injection rate: −68% [6×10^{10} GC/eye] and −61% [1.6×10^{11} GC/eye]).[1] To model the ocular distribution of ABBV-RGX-314 TP, the peak mean ABBV-RGX-314 TP concentration of 643.8 ng/mL observed in cohort 4 (1.6×10^{11} GC/eye) of the phase I/IIa study at 6 months, which received a dose that is closest to the high dose (1.3×10^{11} GC/eye) being evaluated in the 2 ongoing pivotal trials ATMOSPHERE and ASCENT was rounded up to the nearest hundred (700 ng/mL) for simplicity and used as the steady state AH TP concentration in the simulation. Based on this simulation, the estimated retinal ABBV-RGX-314 TP concentration of 5.98 µg/g compared favorably to the C_{trough} of IVT ranibizumab (5.37 µg/g) with monthly 0.5 mg dosing regimen, indicating that this dose level can provide sufficient ABBV-RGX-314 TP coverage in the retina.

Whereas monthly IVT dosing is the approved regimen for ranibizumab for the management of nAMD, a large proportion of patients with nAMD have been reported to follow the PRN or the T&E regimen and receive ranibizumab injections far less frequently.[25,26] In the Intelligent Research in Sight (IRIS) registry, a higher proportion of patients with nAMD received ranibizumab injection intervals of once every 6 to 7 weeks (Q6–7W; 20.0%, 17.9%, and 17.2%) and once every 8 to 9 weeks (Q8–9W; 20.4%, 20.2%, and 20.7%) compared to once every 4 to 5 weeks (Q4–5W; 16.7%, 14.2%, and 15.8%) at the end of year 1, year 2, and year 3,

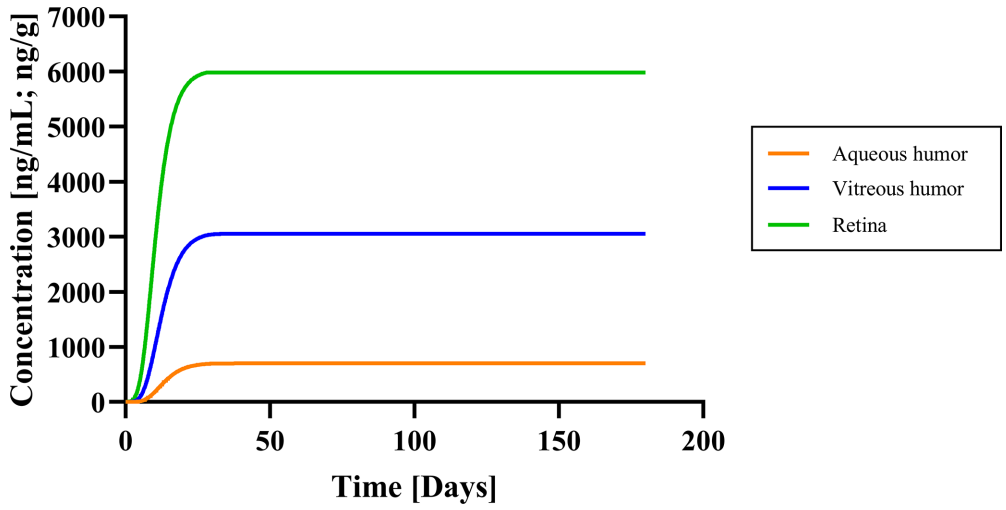

Figure 8. Simulated concentration-time profile of ABBV-RGX-314 TP in the AH, VH, and retina of the human eye following an SR injection of ABBV-RGX-314 at steady-state AH ABBV-RGX-314 TP concentration of 700 ng/mL.

respectively, with once every 8 to 9 week dosing being the most common interval.[27] Similarly, Kiss and colleagues reported mean ranibizumab injection frequencies of 5.62 (n = 1087) and 5.95 (n = 221) over a 12-month period in treatment-naïve and previously treated patients with nAMD, respectively, consistent with once every 8 to 9 week dosing interval reported in the IRIS registry.[28] This suggests that comparing ABBV-RGX-314 TP retinal concentrations (5.98 µg/g) to retinal ranibizumab C_{trough} estimated at day 30 (5.37 µg/g), is likely conservative. Instead, model estimated retinal ranibizumab trough concentration at day 56 following 0.5 mg of IVT bolus administration at 0.718 µg/g may better reflect the actual retinal C_{trough} in patients with nAMD under clinical management in the real-world setting. Hence, AH ABBV-RGX-314 TP concentrations observed at 2 years post-dose at dose levels 6.0×10^{10} GC/eye and 1.6×10^{11} GC/eye with corresponding simulated retinal TP concentrations of 1.94 µg/g and 2.33 µg/g, respectively, are at least 2.7-fold above the ranibizumab day 56 C_{trough} level and demonstrate ABBV-RGX-314 gene therapy achieved and maintained sufficient retinal exposure for up to 2 years. Given that comparable dose levels are being evaluated in pivotal trials, this result supports the potential of those clinical dose levels of ABBV-RGX-314 to provide a more convenient and durable treatment solution compared to the current standard of care, freeing patients from the burden of frequent injections while maintaining therapeutic efficacy.

It is worth noting that there were several limitations in this investigation. First, the current model assumed homogenous retinal transduction and protein expression following SR injection of ABBV-RGX-314. Although the transduction of ABBV-RGX-314 may be limited to the cells in and around the SR injection bleb, given that ABBV-RGX-314 TP is a secreted soluble protein, it is believed to diffuse across the retina upon secretion from the transduced cells but most likely not resulting in uniform retinal drug concentration throughout the tissue. A preclinical biodistribution study suggested a marginal degree of retinal concentration gradient between the bleb (or bleb-adjacent) and the non-bleb area for secreted protein using AAV8 vector similar to ABBV-RGX-314 TP when delivered subretinally (data on file). Therefore, the assumption of homogenous concentration of ABBV-RGX-314 TP across the entire retina to simplify the CFD modeling approach may be reasonable. Second, the model assumed the retinal ABBV-RGX-314 TP concentration to reach steady-state concentration of 5.98 µg/g within 28 days and remains constant through the end of simulation period (day 180). In principle, transgene of an efficient AAV-based gene therapy product persists within the nucleus as episomal DNA, leading to long-term and stable TP expression.[29] Nevertheless, TP expression can diminish over time due to a variety of mechanisms, including target-mediated clearance, immune response against the TP, and cell turnover.[30] Therefore, whereas the simulated retinal ABBV-RGX-314 TP concentration appeared comparable to C_{trough} of monthly IVT 0.5 mg ranibizumab, this level of retinal exposure may not be maintained indefinitely. Third, because the bioanalytical method used to quantify ABBV-RGX-314 TP could not distinguish between ranibizumab and ABBV-RGX-314 TP due to similarities in structures, our model did not consider

the confounding effects of supplemental ranibizumab IVT injections in the AH ABBV-RGX-314 TP data from study RGX-314-001, in which IVT ranibizumab was administered 2 weeks prior to ABBV-RGX-314 administration and as PRN beginning 4 weeks post ABBV-RGX-314 treatment. Last, published clinical AH ranibizumab data by Krohne et al. used to calibrate the CFD model in humans consisted of PK data collected from patients with various retinal diseases, including nAMD, retinal vein occlusion, and diabetic macular edema, due to limited ocular ranibizumab PK data available in humans.[5] It is not clearly understood if or how different retinal diseases or disease severity influence the intraocular PKs of ranibizumab and whether the published values are truly reflective of patients with nAMD, which is the population of interest in this investigation. In addition, sparsity in ocular PK sampling in this study, particularly at earlier timepoints, provided limited information on the earlier portion of the drug concentration-time curve in AH, which may have contributed to poor model fitting.

In conclusion, this ocular CFD model aimed to bridge nonclinical and clinical ranibizumab data to address the lack of ocular ABBV-RGX-314 TP PK data in target tissues in humans. It is an effective approach to link limited human ocular PK data with rich preclinical data to aid MIDD in clinical dose selection. The simulation output from this model supports the doses selected for the ongoing pivotal trials for ABBV-RGX-314.

Acknowledgments

The authors thank Francisco J. Lopez, MD, PhD, Group Medical Director, Clinical Development Eye Care, AbbVie, for his scientific insights and feedback on this manuscript.

Supported by AbbVie, for the design, study conduct, and financial support for this research. AbbVie also participated in the interpretation of data, review, and approval of the publication.

Disclosure: **J. Park**, AbbVie (E); **M. Tamhane**, AbbVie (E); **J. Shen**, AbbVie (E); **M. Kazemi**, AbbVie (C)

References

1. Campochiaro PA, Avery R, Brown DM, et al. Gene therapy for neovascular age-related macular degeneration by subretinal delivery of RGX-314: a phase 1/2a dose-escalation study. *Lancet*. 2024;403:1563–1573.
2. Nowak JZ. Age-related macular degeneration (AMD): pathogenesis and therapy. *Pharmacol Rep*. 2006;58:353–363.
3. Ding X, Patel M, Chan CC. Molecular pathology of age-related macular degeneration. *Prog Retin Eye Res*. 2009;28:1–18.
4. Tan CS, Ngo WK, Chay IW, Ting DS, Sadda SR. Neovascular age-related macular degeneration (nAMD): a review of emerging treatment options. *Clin Ophthalmol*. 2022;16:917–933.
5. Krohne TU, Liu Z, Holz FG, Meyer CH. Intraocular pharmacokinetics of ranibizumab following a single intravitreal injection in humans. *Am J Ophthalmol*. 2012;154:682–686.e2.
6. Do DV, Rhoades W, Nguyen QD. Pharmacokinetic study of intravitreal aflibercept in humans with neovascular age-related macular degeneration. *Retina*. 2020;40:643–647.
7. Celik N, Scheuerle A, Auffarth GU, Kopitz J, Dithmar S. Intraocular pharmacokinetics of aflibercept and vascular endothelial growth factor-A. *Invest Ophthalmol Vis Sci*. 2015;56:5574–5578.
8. Wykoff CC, Campochiaro PA, Pieramici DJ, et al. Pharmacokinetics of the port delivery system with ranibizumab in the Ladder Phase 2 Trial for Neovascular Age-Related Macular Degeneration. *Ophthalmol Ther*. 2022;11:1705–1717.
9. Missel PJ, Horner M, Muralikrishnan R. Simulating dissolution of intravitreal triamcinolone acetonide suspensions in an anatomically accurate rabbit eye model. *Pharm Res*. 2010;27:1530–1546.
10. Power ED. A nonlinear finite element model of the human eye to investigate ocular injuries from night vision goggles. *Virginia Tech*. Published online April 20, 2001. Available at: https://vtechworks.lib.vt.edu/items/e16e0706-967a-4085-84df-71358b23d14b.
11. Faqi AS. A comprehensive guide to toxicology in preclinical drug development. *Chapter 24 - Safety Evaluation of Ocular Drugs, Academic Press*, 2013:567–617. doi:10.1016/b978-0-12-387815-1.00024-1.
12. Gaudreault J, Fei D, Rusit J, Suboc P, Shiu V. Preclinical pharmacokinetics of ranibizumab (rhuFabV2) after a single intravitreal administration. *Invest Ophthalmol Vis Sci*. 2005;46:726–733.
13. Chowdhury EA, Meno-Tetang G, Chang HY, et al. Current progress and limitations of AAV mediated delivery of protein therapeutic genes and the importance of developing quantitative phar-

macokinetic/pharmacodynamic (PK/PD) models. *Adv Drug Deliv Rev*. 2021;170:214–237.
14. Prasad KMR, Xu Y, Yang Z, Toufektsian MC, Berr SS, French BA. Topoisomerase inhibition accelerates gene expression after adeno-associated virus-mediated gene transfer to the mammalian heart. *Mol Ther*. 2007;15:764–771.
15. Torres JF, Komiya A, Okajima J, Maruyama S. Measurement of the molecular mass dependence of the mass diffusion coefficient in protein aqueous solutions. *Defect and Diffusion Forum*. 2012;326–328:452–458.
16. LUCENTIS (ranibizumab injection) [package insert]. *US Food and Drug Administration website*. Available at: https://www.accessdata.fda.gov/drugsatfda_docs/label/2018/125156s117lbl.pdf.
17. Hutton-Smith LA, Gaffney EA, Byrne HM, Maini PK, Schwab D, Mazer NA. A mechanistic model of the intravitreal pharmacokinetics of large molecules and the pharmacodynamic suppression of ocular vascular endothelial growth factor levels by ranibizumab in patients with neovascular age-related macular degeneration. *Mol Pharm*. 2016;13:2941–2950.
18. Balachandran RK, Barocas VH. Computer modeling of drug delivery to the posterior eye: effect of active transport and loss to choroidal blood flow. *Pharm Res*. 2008;25:2685–2696.
19. Tojo K, Isowaki A. Pharmacokinetic model for in vivo/in vitro correlation of intravitreal drug delivery. *Adv Drug Deliv Rev*. 2001;52:17–24.
20. Ford JL, Karatza E, Mody H, et al. Clinical pharmacology perspective on development of adeno-associated virus vector-based retina gene therapy. *Clin Pharmacol Ther*. 2024;115:1212–1232.
21. Madabushi R, Seo P, Zhao L, Tegenge M, Zhu H. Review: Role of model-informed drug development approaches in the lifecycle of drug development and regulatory decision-making. *Pharm Res*. 2022;39:1669–1680.
22. Madabushi R, Benjamin J, Zhu H, Zineh I. The US Food and Drug Administration's Model-Informed Drug Development Meeting Program: From Pilot to Pathway. *Clin Pharmacol Ther*. 2024;116:278–281.
23. Silva R, Berta A, Larsen M, Macfadden W, Feller C, Monés J. Treat-and-extend versus monthly regimen in neovascular age-related macular degeneration: results with ranibizumab from the TREND study. *Ophthalmology*. 2018;125:57–65.
24. Augsburger M, Sarra GM, Imesch P. Treat and extend versus pro re nata regimens of ranibizumab and aflibercept in neovascular age-related macular degeneration: a comparative study. *Graefes Arch Clin Exp Ophthalmol*. 2019;257:1889–1895.
25. Ferreira A, Sagkriotis A, Olson M, Lu J, Makin C, Milnes F. Treatment frequency and dosing interval of ranibizumab and aflibercept for neovascular age-related macular degeneration in routine clinical practice in the USA. *PLoS One*. 2015;10:e0133968.
26. Urbano CA, Maatouk C, Greenlee T, et al. Real-world treatment patterns in a population with neovascular AMD treated with anti-VEGF agents. *Ophthalmic Surg Lasers Imaging Retina*. 2021;52:190–198.
27. MacCumber MW, Yu JS, Sagkriotis A, et al. Antivascular endothelial growth factor agents for wet age-related macular degeneration: an IRIS registry analysis. *Can J Ophthalmol*. 2023;58:252–261.
28. Kiss S, Malangone-Monaco E, Wilson K, et al. Real-world injection frequency and cost of ranibizumab and aflibercept for the treatment of neovascular age-related macular degeneration and diabetic macular edema. *J Manag Care Spec Pharm*. 2020;26:253–266.
29. Wang D, Tai PWL, Gao G. Adeno-associated virus vector as a platform for gene therapy delivery. *Nat Rev Drug Discov*. 2019;18:358–378.
30. Muhuri M, Levy DI, Schulz M, McCarty D, Gao G. Durability of transgene expression after rAAV gene therapy. *Mol Ther*. 2022;30:1364–1380.